

## Supporting Information

### Spin-Orbit Charge-Transfer Intersystem Crossing in Heavy-Atom-Free Orthogonal Covalent Boron-Dipyrromethene Heterodimers

Zeming Wang,<sup>1#</sup> Lin Ma,<sup>1#</sup> Hongmei Zhao,<sup>1</sup> Yan Wan,<sup>3</sup> Xian-Fu Zhang,<sup>\*2</sup> Yang Li,<sup>\*1</sup> Zhuoran  
Kuang,<sup>\*1</sup> Andong Xia<sup>1</sup>

1. State Key Laboratory of Information Photonic and Optical Communications, and School of  
Science, Beijing University of Posts and Telecommunications (BUPT), Beijing 100876, P. R.  
China

2. Department of Materials Science and Engineering, Southern University of Science and  
Technology, Shenzhen, Guangdong Province 518055, P. R. China

3. College of Chemistry, Beijing Normal University, Beijing 100875, P. R. China

# Z.W. and L.M. contributed equally to this work.

#### Contents

S1. Material and Methods.....	2
S2. Supplementary Stationary Spectroscopy .....	3
S3. Transient absorption spectra of Monomeric BODIPY .....	4
S4. Transient absorption spectra of Dimeric BODIPY and Global Analysis.....	5
S5. TD-DFT Calculation and Electron Excitation Analysis .....	8
S6. Supplementary References .....	9

## S1. Material and Methods

**Chemicals.** The *meso*- $\beta$  linked BODIPY dimers<sup>1</sup> and BODIPY monomer<sup>2</sup> were synthesized as previously reported. For spectroscopic studies, BODIPY dimers and monomer were dissolved in the appropriate solvents. Solvents utilized in this work were obtained from Concord Technology (HPLC grade).

**Steady-State Measurements.** Absorption spectra were measured on a spectrophotometer U-3900 (Hitachi, Japan), with an optical density between 0.15 and 0.3 at the peak of the lowest absorption band. Fluorescence spectra were measured on a spectrometer F-4600 (Hitachi, Japan). For fluorescence measurements, the absorbance of the solutions at the band maximum was around 0.1 OD over 1 cm light path.

**Femtosecond Transient Absorption Measurements.** Femtosecond time-resolved transient absorption spectra were measured with a commercial transient absorption spectrometer (Harpia-TA, Light Conversion). Briefly, fundamental pulses are derived from an amplified femtosecond Ti:sapphire laser (Astrella, Coherent). The laser delivers 40 fs pulses at 1 kHz and the output is split for white-light continuum generation and optical pumping. The white-light continuum is used as broadband optical probe from the near-UV to the near-infrared. It is generated by focusing the fundamental laser beam onto a 2 mm thick CaF<sub>2</sub> plate, which is oriented and continuously shifted in perpendicular directions. The required pumping pulse is obtained by an optical parametric amplifier (TOPAS-C, Light Conversion). The polarization of the pump beam was set to the magic angle (55°) relative to the probe beam. Transient absorption is calculated from consecutive pump-on and pump-off measurements and averaged over 1000 shots. UV-Vis absorption spectra of the samples are measured before and after every measurement in a spectrophotometer. No significant photo-degradation was observed after femtosecond measurements. The femtosecond time-resolved differential absorbance data were analyzed by using R-package TIMP software with the graphical interface Glotaran<sup>3</sup> and CarpetView (Light Conversion). In the global target analysis, the differential absorbances  $\Delta A(t, \lambda)$  are decomposed as a superposition of several principal spectral components  $\varepsilon_i(\lambda)$  weighed by their concentrations  $c_i(t)$ :<sup>4</sup>

$$\Delta A(t, \lambda) = \sum_{i=1}^n c_i(t) \varepsilon_i(\lambda). \quad (1)$$

**Quantum calculation.** The calculations were carried out using density functional theory (DFT) and time-dependent DFT (TD-DFT) method as implemented with high-nonlocality hybrid functional, M06-2X,<sup>5</sup> was chosen together with a 6-311G(d,p) basis set<sup>6</sup> for geometry optimization and excitation energy calculations. In all the cases, frequency analysis was made after geometry optimization to ensure convergence to an energy minimum. D3 version of Grimme's dispersion with the original D3 damping function was applied during the geometrical optimization and excitation energy calculations.<sup>7</sup> All simulations were implemented for isolated molecules using the Gaussian 16 software package.<sup>8</sup> Electronic excitation analysis and visualization of electron-hole density were conducted by the Multiwfn software.<sup>9</sup> The spin-orbit coupling (SOC) matrix elements between the excited states were calculated by the TD-DFT at the M06-2X/6-311G(d,p) level without Tamm-Dancoff approximation on the optimized S<sub>0</sub> and S<sub>1</sub> geometries using ORCA 5.0 program package.<sup>10</sup>

## S2. Supplementary Stationary Spectroscopy

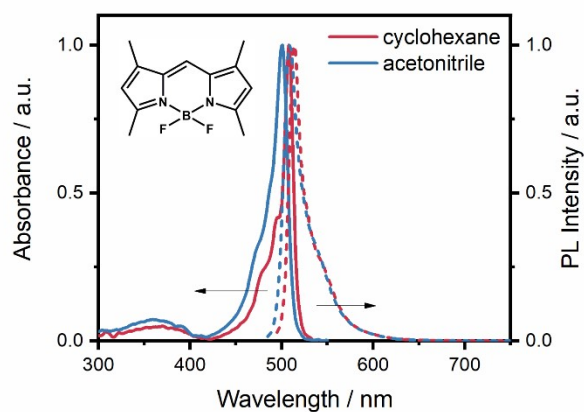


**Figure S1.** Steady-state absorption and emission spectra of monomeric BODIPY in cyclohexane and acetonitrile. The chemical structure of monomeric BODIPY was shown in the inset.

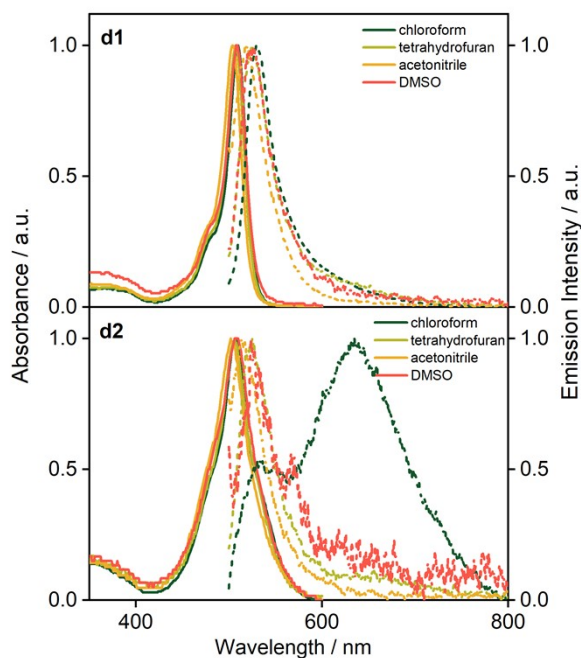


**Figure S2.** The supplementary intensity-normalized stationary absorption and emission spectra of **d1** and **d2** in solvents at room temperature. Solid and dotted curves represent absorption and emission spectra, respectively.

**Table S1.** Fluorescence Quantum Yield of Dimeric BODIPY **d1** and **d2** in Cyclohexane ( $\epsilon = 2.02$ ), Toluene ( $\epsilon = 2.37$ ), Chloroform ( $\epsilon = 4.71$ ), Tetrahydrofuran (THF,  $\epsilon = 7.42$ ), Dichloromethane (DCM,  $\epsilon = 8.93$ ), Acetonitrile ( $\epsilon = 35.69$ ), and Dimethyl Sulfoxide (DMSO,  $\epsilon = 46.82$ ).<sup>11</sup>

<b>Compound</b>	<b>Solvent</b>	<b>Fluorescence Quantum Yield</b>
<b>d1</b>	cyclohexane	0.82
	toluene	0.51
	chloroform	0.09
	THF	0.03
	DCM	0.020
	acetonitrile	0.019
	DMSO	0.011
<b>d2</b>	cyclohexane	0.61
	toluene	0.08
	chloroform	0.013
	THF	0.020
	DCM	0.004
	acetonitrile	0.010
	DMSO	0.003

### S3. Transient absorption spectra of Monomeric BODIPY

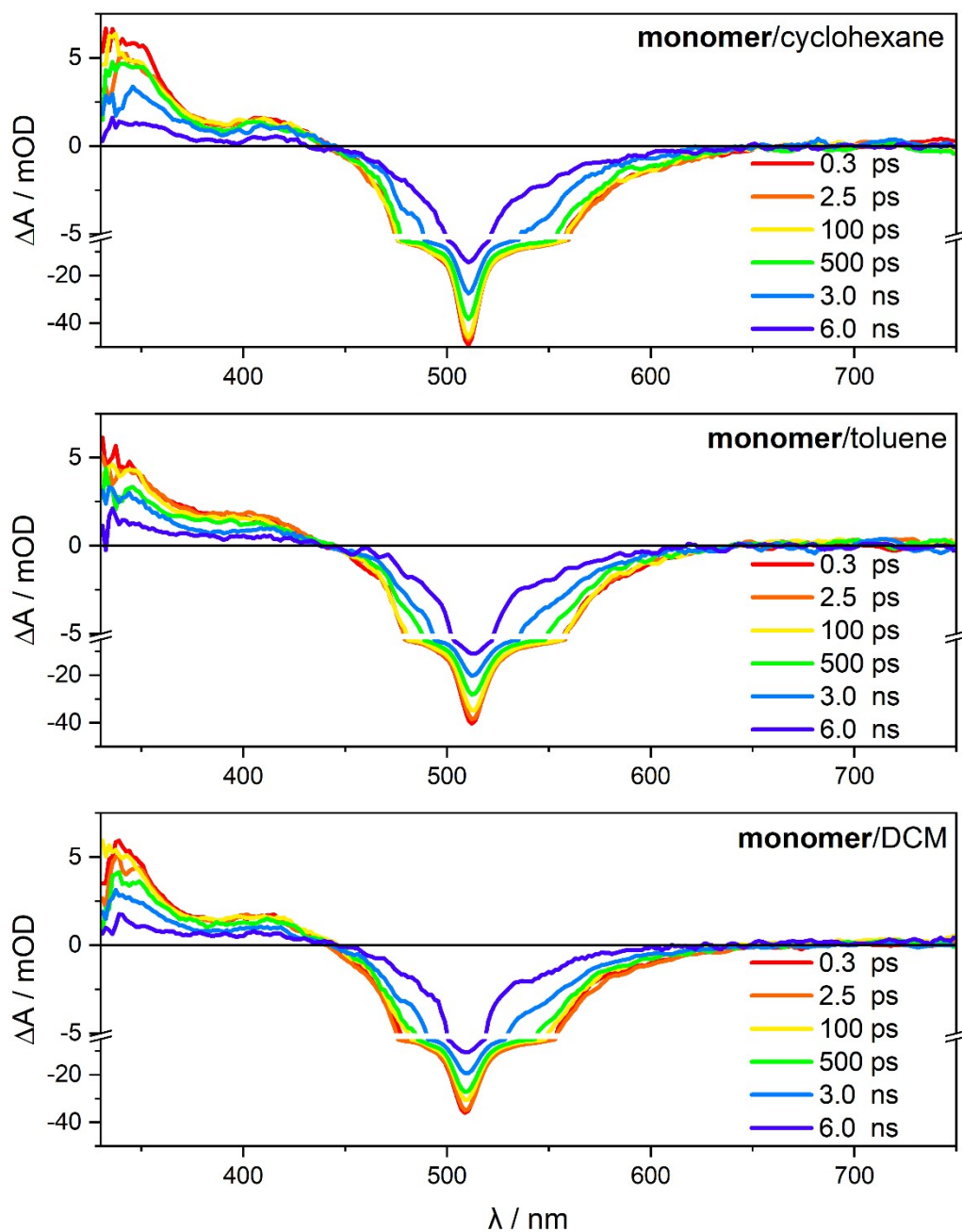


**Figure S3.** Femtosecond TA spectra of monomeric BODIPY. Experimental conditions:  $\lambda_{\text{ex}} = 515$  nm; solvent: cyclohexane, toluene, and dichloromethane (DCM).

## S4. Transient absorption spectra of Dimeric BODIPY and Global Analysis

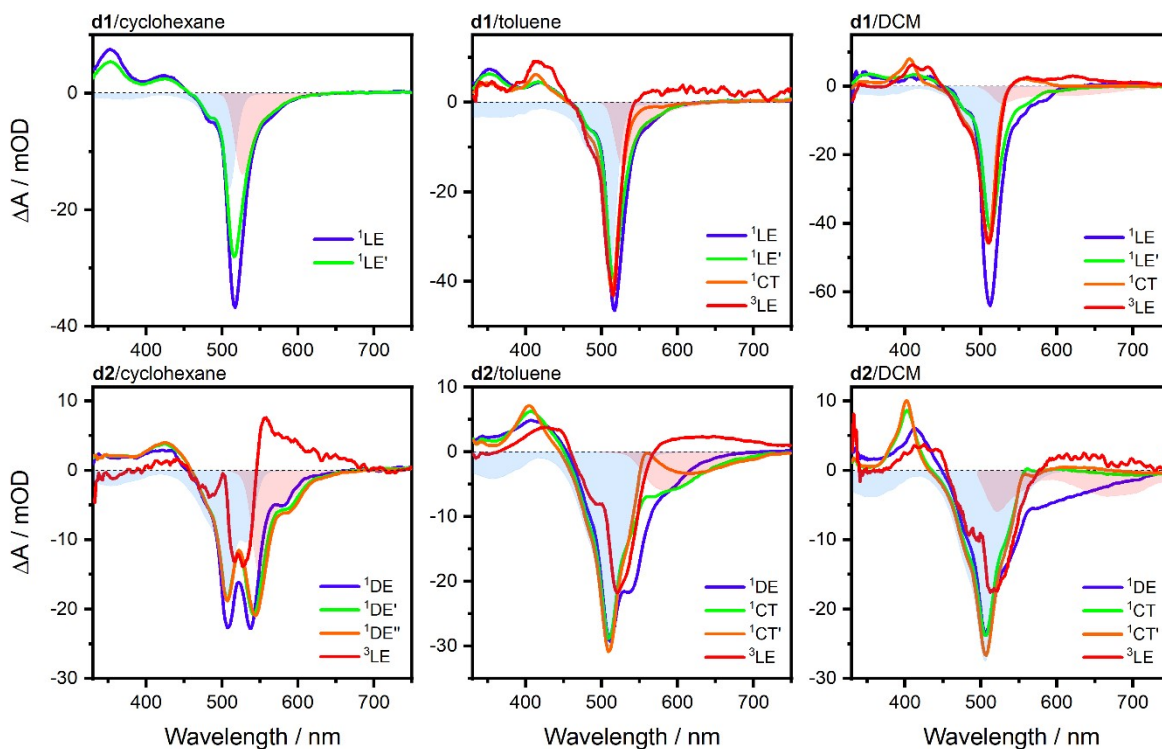


**Figure S4.** The species-associated different spectra (SADS) of dimeric BODIPY **d1** and **d2** in cyclohexane, toluene, and dichloromethane (DCM) obtained from global target analysis. For better identification of GSB and SE features in the SADS, scaled stationary absorption and emission spectra are shown with blue and red shaded areas, respectively. LE: localized-excitation state, LE'/LE'': conformational-relaxed LE state, DE: delocalized-excitation state, DE'/DE'': conformational-relaxed DE state, CT: charge-transfer state, and GS: ground state.

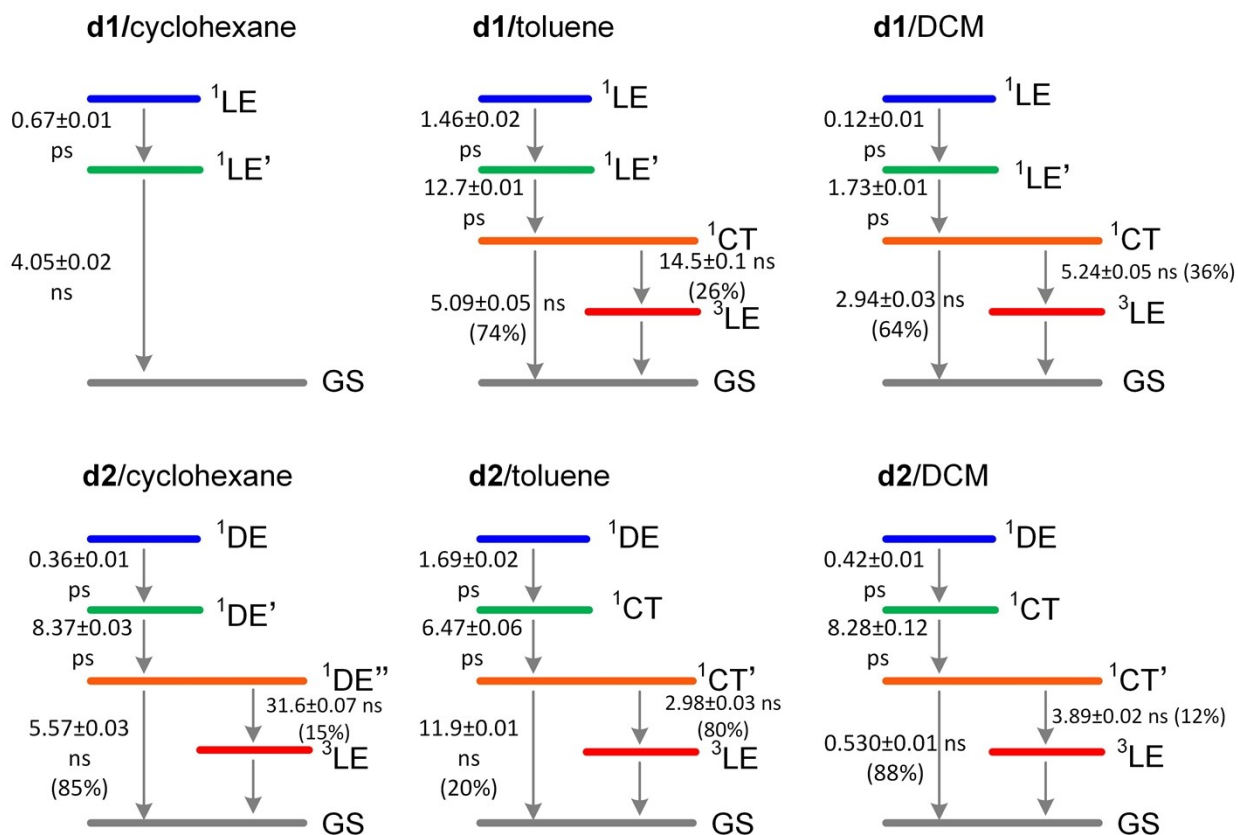


**Figure S5.** The species assignments and the associated reaction rate constants of the species-associated different spectra (SADS) of dimeric BODIPY **d1** and **d2** in cyclohexane, toluene, and dichloromethane (DCM) obtained from global target analysis. LE: localized-excitation state, LE'/LE'': conformational-relaxed LE state, DE: delocalized-excitation state, DE'/DE'': conformational-relaxed DE state, CT: charge-transfer state, and GS: ground state.

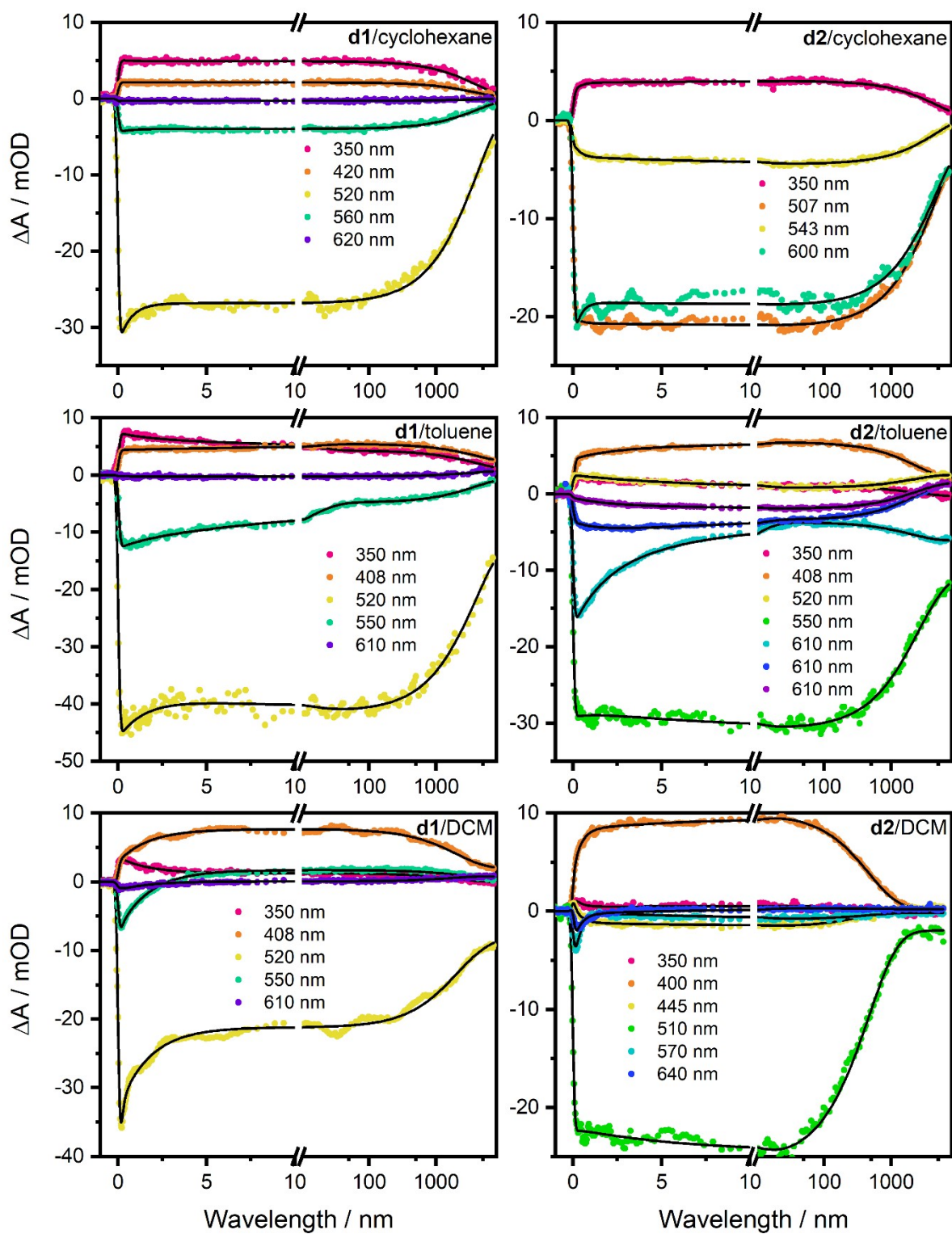


**Figure S6.** The fitting results of representative wavelength in the global target analysis of dimeric BODIPY **d1** and **d2** in cyclohexane, toluene, and dichloromethane (DCM) for showing the fitting quality.

## S5. TD-DFT Calculation and Electron Excitation Analysis

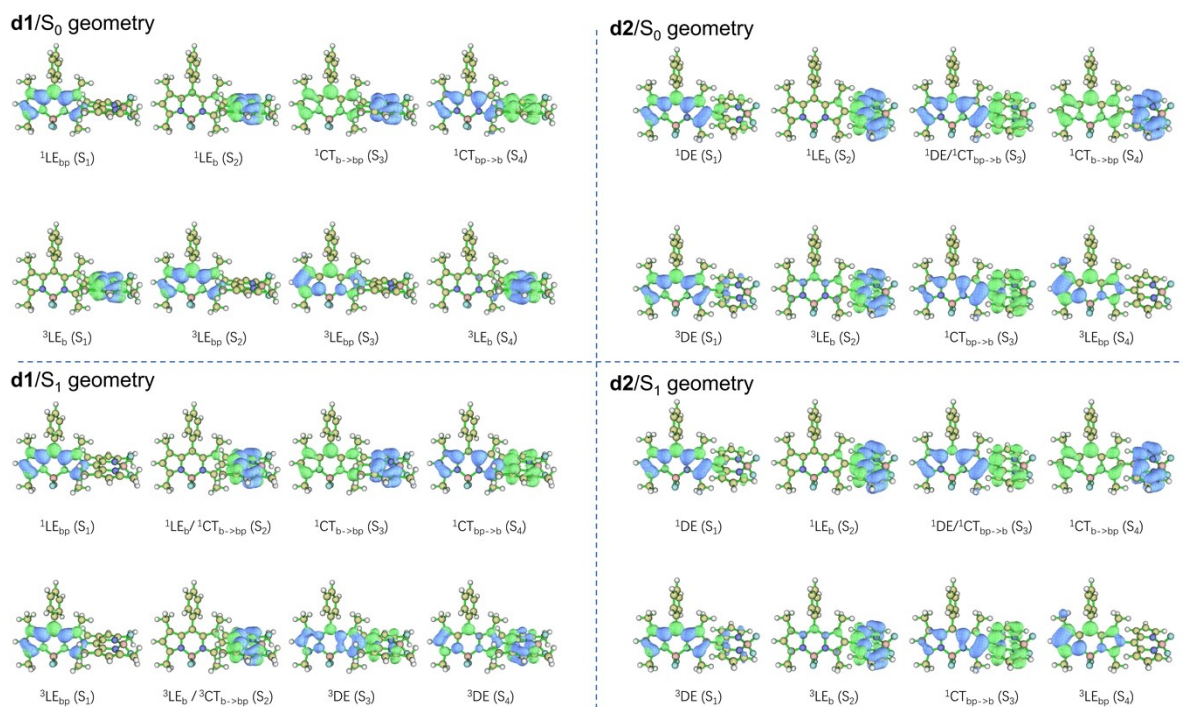


**Figure S7.** Electronic excitation analysis of the lowest lying singlet excited states of the dimeric BODIPY **d1** and **d2** in the optimized S<sub>0</sub> and S<sub>1</sub> geometries. Blue and green isosurfaces represent hole and electron distributions, respectively.

## S6. Supplementary References

1. X.-F. Zhang, X. Yang and B. Xu, PET-based bisBODIPY photosensitizers for highly efficient excited triplet state and singlet oxygen generation: tuning photosensitizing ability by dihedral angles, *Phys. Chem. Chem. Phys.*, 2017, **19**, 24792-24804.
2. W. Pang, X.-F. Zhang, J. Zhou, C. Yu, E. Hao and L. Jiao, Modulating the singlet oxygen generation property of meso- $\beta$  directly linked BODIPY dimers, *Chem. Commun.*, 2012, **48**, 5437-5439.
3. J. J. Snellenburg, S. P. Liptenok, R. Seger, K. M. Mullen and I. H. M. v. Stokkum, Glotaran: A Java-Based Graphical User Interface for the R Package TIMP, *J. Stat. Soft.*, 2012, **49**, 1-22.
4. I. H. M. van Stokkum, D. S. Larsen and R. van Grondelle, Global and target analysis of time-resolved spectra, *Biochim. Biophys. Acta*, 2004, **1657**, 82-104.
5. Y. Zhao and D. G. Truhlar, The M06 suite of density functionals for main group thermochemistry, thermochemical kinetics, noncovalent interactions, excited states, and transition elements: two new functionals and systematic testing of four M06 functionals and 12 other functionals, *Theor. Chem. Acc.*, 2008, **119**, 525-525.
6. R. Krishnan, J. S. Binkley, R. Seeger and J. A. Pople, Self - consistent molecular orbital methods. XX. A basis set for correlated wave functions, *J. Chem. Phys.*, 1980, **72**, 650-654.
7. S. Grimme, J. Antony, S. Ehrlich and H. Krieg, A consistent and accurate ab initio parametrization of density functional dispersion correction (DFT-D) for the 94 elements H-Pu, *J. Chem. Phys.*, 2010, **132**, 154104.
8. M. J. Frisch, G. W. Trucks, H. B. Schlegel, G. E. Scuseria, M. A. Robb, J. R. Cheeseman, G. Scalmani, V. Barone, G. A. Petersson, H. Nakatsuji, X. Li, M. Caricato, A. V. Marenich, J. Bloino, B. G. Janesko, R. Gomperts, B. Mennucci, H. P. Hratchian, J. V. Ortiz, A. F. Izmaylov, J. L. Sonnenberg, Williams, F. Ding, F. Lipparini, F. Egidi, J. Goings, B. Peng, A. Petrone, T. Henderson, D. Ranasinghe, V. G. Zakrzewski, J. Gao, N. Rega, G. Zheng, W. Liang, M. Hada, M. Ehara, K. Toyota, R. Fukuda, J. Hasegawa, M. Ishida, T. Nakajima, Y. Honda, O. Kitao, H. Nakai, T. Vreven, K. Throssell, J. A. Montgomery Jr., J. E. Peralta, F. Ogliaro, M. J. Bearpark, J. J. Heyd, E. N. Brothers, K. N. Kudin, V. N. Staroverov, T. A. Keith, R. Kobayashi, J. Normand, K. Raghavachari, A. P. Rendell, J. C. Burant, S. S. Iyengar, J. Tomasi, M. Cossi, J. M. Millam, M. Klene, C. Adamo, R. Cammi, J. W. Ochterski, R. L. Martin, K. Morokuma, O. Farkas, J. B. Foresman and D. J. Fox, Gaussian 16 Rev. A.03, *Journal*, 2016.
9. T. Lu and F. Chen, Multiwfn: A multifunctional wavefunction analyzer, *J. Comput. Chem.*, 2012, **33**, 580-592.
10. F. Neese, Software update: The ORCA program system—Version 5.0, *WIREs Computational Molecular Science*, 2022, **12**, e1606.
11. Y. Marcus, *The Properties of Solvents*, Wiley, 1998.